JOURNAL OF THE BALKAN GEOPHYSICAL SOCIETY, Vol. 2, No 4, November 1999, p. 100-111, 10 figs.

# Detecting small-scale targets by the two-sided gradient transformation

M. Emin Candansayar [*] , Ahmet T. Basokur [*] and Ertan Peksen [* *]

[*] Ankara Universitesi, Fen Fakultesi, Jeofizik Muh. B., Tandogan, 06100 Ankara, Turkey.

E-mails: candansa@science.ankara.edu.tr; basokur@science.ankara.edu.tr

[* *] Univ. of Utah, Dept. of Geology and Geophysics, 717WBB, Salt Lake City, USA.
E-mail: epeksen@mines.utah.edu

( Received 21 July 1999; accepted 30 September 1999 )

***Abstract:*** *The two-sided three-electrode arrangement uses equally spaced electrodes permitting the use of automated devices for fast measurements. A new transformation method named as the 'two-sided gradient' (TSG) is derived by a modification of the gradient (G) transformation of Karous and Pernu(1985). The gradient transformations may remove the contribution of the 1-D earth from the apparent resistivity data, improving thus the effect of the lateral resistivity variation. This helps to the fast detection of small-scale targets. Tests on synthetic data show that the TSG transformation is superior to the G transformation in delineating the shallow lateral discontinuities. However, both transformations do not provide estimates for the depth and the exact size of the target.*

*A field application was carried out in the archaeological site known as 'Alacahoyuk', a religious site of Hittites hosting the ruins of temples. The two-dimensional inversion of the two-sided three-electrode apparent resistivity data lead to the location of a part of the city-wall. The archaeological excavation next unearthed the wall. Thus, the validity of our interpretation was checked. The 2-D inversion of the two-sided three-electrode data estimated correctly the location, the depth and the dimensions of the city-wall. The 2-D inversion results predicted the termination of the wall inferred by the results in some profiles. On the contrary, the TSG transformation indicated the continuation of the city-wall and the subsequent excavations proved this fact. The field survey proved that the TSG transformation is a fast and efficient method in delineating small-scale targets. Then, it can be used as a complementary method for the 2-D inversion methods.*

***Key Words:*** *Small-scale Targets, Two-sided Gradient Transformation, Archaeological Survey.*

## INTRODUCTION

The direct current method and the magnetics comprise the main tools in archaeological geophysics. The direct current method is used to locate targets such as ruins of foundation walls, tombs. Buried archaeological structures, such as walls constructed by stones or bricks and roads made of stone or gravel, have usually higher resistivity values than that of the hosting soil. Voids and tombs pose also higher resistivity values than the surrounding soil. Also the corridors, buried inside tumuli, show sometimes-higher resistivity than the hosting medium.

Currently, the two-dimensional (2-D) inversion of the apparent resistivity data is the standard scheme for the estimation of the burial depth and the dimensions of the archaeological targets (Noel and Walker, 1990; Noel and Xu 1991; Griffiths and Barker, 1994). However, the application of the method requires a careful mesh design and the 2-D model response computations which are performed to update the initial model are time consuming. For these reasons,

the inversion of the data is usually performed after the fieldwork has been completed.

Among many others, the cross-correlation method (Orlando et al., 1987; Bernabini *et al*., 1988; Brizollari et al. 1989,1992) and the inverse filtering (Tsokas and Tsourlos, 1997) are good examples of fast operations to locate the archaeological targets. Kampke (1999) has suggested another type of data processing technique named as "focused imaging". The technique is applied to apparent resistivity data measured along a profile. The outcome of this imaging scheme shows only the location of the buried target.

Besides the data processing techniques used to aid the interpretation, the type of electrode configuration used for the data acquisition is also important to detect the small scale targets. For example, Karous and Pernu(1985) has suggested a combined sounding-profiling measurement with the three-electrode array for the detection of thin conductors. This method is consisting in measuring simultaneously, two half-Schlumberger arrays, which use the same potential electrode pair. Schulz and Tezkan (1988) have also pointed out the superior resolving ability of the two-sided half-Schlumberger array. Karous and Pernu (1985) introduced a fast and approximate data processing technique named as 'gradient (G) transformation' to detect thin conductors.

The half-Schlumberger array is not a practical data acquisition technique for shallow investigations such as the case of archaeological prospecting. Nowadays, the widely employed multi-electrode systems use the equally spaced electrodes, allowing thus, fast data acquisition (Van Overmeeren and Ritsema, 1988; Dahlin, 1996). Candansayar and Basokur (2000) have suggested a two-sided three-electrode system that uses equally spaced electrodes in order to overcome the difficulties encountered in the data acquisition,. They showed the superiority of the method for the detection of small-scale targets over their four-electrode counterparts by examining the 2-D inversion results of both types of apparent resistivity data. The 2-D inversion of the two-sided three-electrode apparent resistivity data accurately determines the size, burial depth and location of the target. However, the in situ processing of the data may be impossible because of the required computation time. It is evident that an approximate and fast method is needed for the preliminary evaluation of the survey. We attempted to use the gradient (G) transformation of Karous and Pernu (1985) for the fast processing of the two-sided three-electrode apparent resistivity data. However, this transformation did not produced satisfactory results for the two-sided three-electrode arrangement. For this reason, we have developed a new data processing technique named as "Two-Sided Gradient" (TSG) transformation that is obtained from the G transformation including some extra terms. This paper compares the results of G and TSG transformations for synthetic and actual field data collected in an archaeological site. The previous 2-D inversion results and the findings of the excavation are used as the reference information for these comparisons.

## DESCRIPTION OF THE TWO-SIDED THREE-ELECTRODE SYSTEM

The electrodes are laid out at equal distances, each from the other, along a measuring profile in order to achieve efficient use of the automated reading systems. This particular lay out of the two-sided three-electrode array is demonstrated in Figure 1. The letters A, B and C represent the current electrodes whilst M and N show the location of the potential electrodes. Any consecutive two electrodes can be used to measure a potential difference. The current electrodes A and B are located at the left- and right-hand sides of a pair of potential electrodes respectively, while the electrode denoted by the letter C is located along the line perpendicular to the centre of the measuring profile. The potential contributed by this source at the electrodes M and N is relatively small if the electrode C is fixed at an adequate distance that is practically considered as being infinite. Two measurement sequences are performed for each position of potential electrodes. The first series of apparent resistivity measurements are conducted by applying a current into ground through the C and $A_1, A_2, ...A_n$ electrodes. The measurements are repeated in the same way by using the C and $B_1, B_2, ...B_n$ electrodes. The apparent resistivity values measured by using C - $A_j$ and C - $B_j$ current electrodes in pairs constitute left and right apparent resistivity values corresponding to the same potential electrode pair (M and N). Shifting the potential electrodes to the next electrode locations and repeating the same measuring sequence, a set of apparent resistivity values along the measuring line is acquired.

The apparent resistivity $\rho_{aA}$ can be defined as

$$\rho_{aA} = k_A \frac{\Delta V_{AMN}}{I} , \qquad (1)$$

where $\Delta V_{AMN}$, is the potential difference between M and N electrodes caused by the current (I) applied through the source (A) and sink (C) electrodes. The geometric factor, $k_A$, of the array is given by

$$k_A = 2\pi a\, n\,(n+1), \qquad n=1, 2,\ldots \qquad (2)$$

where *a* is the distance between two consecutive electrodes.

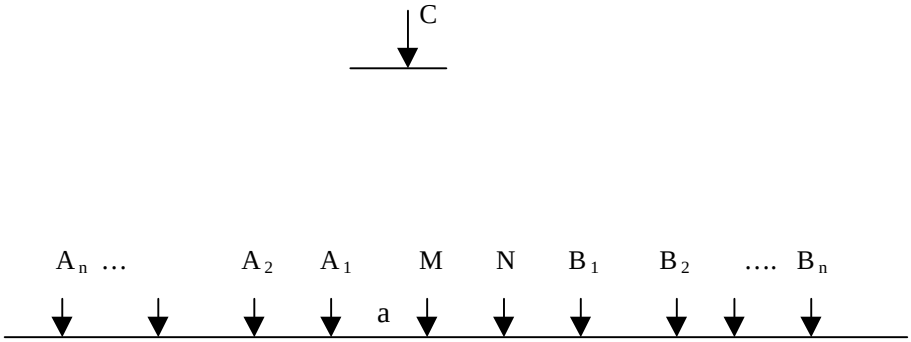


**FIG. 1.** Field layout of the two-sided three-electrode measurement system. *A* and *B* denote the current electrodes. *C* is the current electrode located at a distant place. *M* and *N* are the potential electrodes. *O* shows the array centre and *a* is the distance between two consecutive electrodes.

The apparent resistivity $\rho_{aB}$ corresponding to the case where the current is applied through B and C electrodes is obtained in a similar way as

$$\rho_{aB} = k_B \frac{\Delta V_{MNB}}{I}, \tag{3}$$

where the geometric factor $k_B$ is equal to

$$k_B = 2\pi a\, n\,(n+1). \tag{4}$$

Considering the conventional application where the current injected through A and B electrodes, the following equations can be obtained for the apparent resistivity $\rho_{aAB}$ and the geometric factor $k_{AB}$

$$\rho_{aAB} = k_{AB} \frac{\Delta V_{MN}}{I}, \tag{5}$$

and

$$k_{AB} = \pi a\, n\,(n+1). \tag{6}$$

Since

$$2k_{AB} = k_A = k_B, \tag{7}$$

then the apparent resistivity $\rho_{AB}$ can be computed from the two other apparent resistivity values. This is a direct implication of the superposition rule without actually measuring the potential difference (Karous and Pernu, 1985). After some algebraic manipulations, equation (7) yields

$$\rho_{aAB} = \frac{\rho_{aA} + \rho_{aB}}{2}. \tag{8}$$

thus, the resistivity $\rho_{aAB}$ can be named as "average apparent resistivity".

## G AND TSG TRANSFORMATIONS

The discrepancy between the apparent values obtained from the corresponding AMN and BMN configurations may be used to locate a resistivity inhomogeneity along the profile direction. The elimination of the effect of 1-D earth may magnify the resistivity variation in the horizontal direction. For this purpose, Karous and Pernu (1985) defined the gradient transformation as

$$G^{i}(x) = \frac{\rho^{i}{}_{aA}(x)}{\rho^{i+1}{}_{aA}(x)} + \frac{\rho^{i}{}_{aB}(x)}{\rho^{i-1}{}_{aB}(x)} - 2 \quad (i = 2, 3, \cdots, L-1), \tag{9}$$

where, *x* is the spacing along the profile and *L* denotes the key numbers of measurement stations. All apparent resistivity values in equation (9) are measured for the same $\overline{AO} = \overline{BO}$ spacing. Since the apparent resistivity values are equal to each other for 1-D earth, the value of G becomes zero for this case. However, the value of G increases or decreases when the discrepancy between the apparent values measured by the AMN and BMN configurations increase. Thus, the value of G becomes proportional to the variation of the resistivity in the horizontal direction.

Karous and Pernu (1985) developed the G transformation for the half-Schlumberger array, which can be applied to all type of three-electrode arrangements. However, our experiences with the two-sided three-electrode array show that the maximum of the G transformation does not always coincide with the location of the target body and the G transformation is not useful for distinguishing closely located targets. For these reasons, we have modified the G transformation to obtain more satisfactory results. The

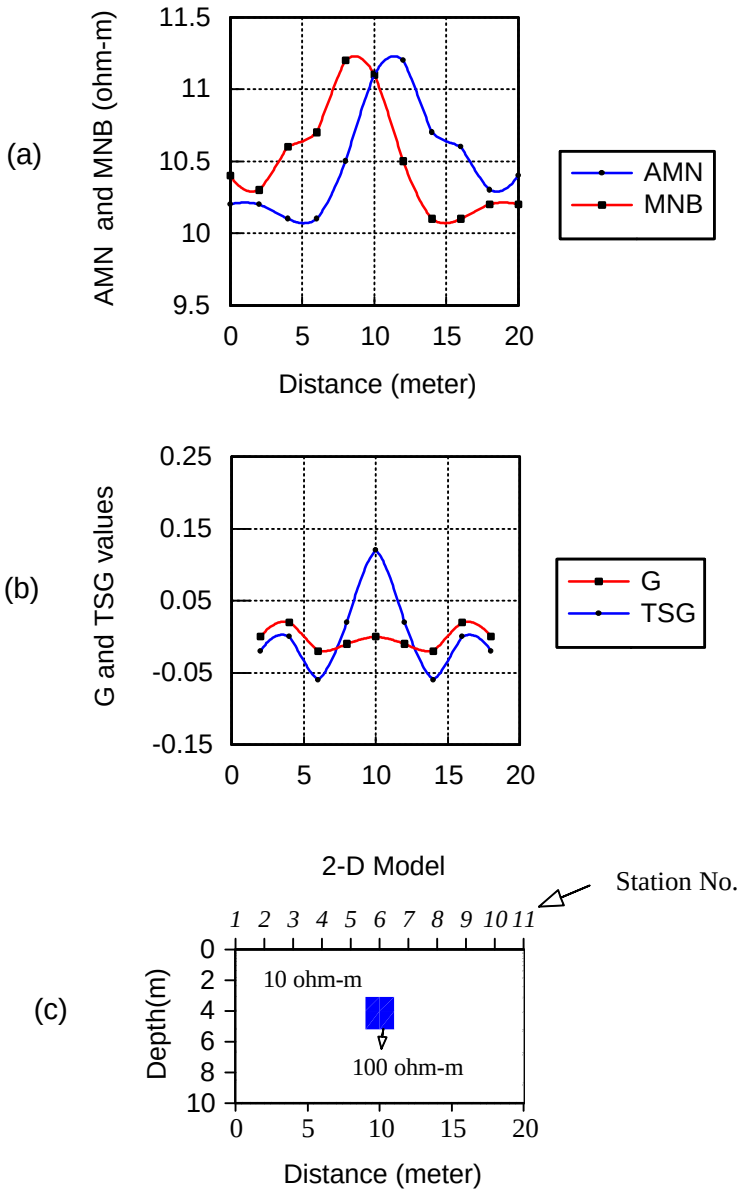


**FIG. 2.** (a) A plot of AMN and BMN apparent resistivity data measured for AB/2=13 m and a=2 m over a resistive buried target. (b) G and TSG plotting versus distance. (c) The two-dimensional model used for the calculation of the synthetic apparent resistivity data by the finite-element method. The target is buried at a depth of 3.11 m into a homogenous medium.

new expression named as Two-Sided Gradient (TSG) transformation uses more apparent resistivity values for the better definition of the inhomogeneity in the horizontal direction and it is given by

$$TSG^{i}(x) = \frac{\rho^{i}_{aA}(x)}{\rho^{i+1}_{aA}(x)} + \frac{\rho^{i}_{aB}(x)}{\rho^{i-1}_{aB}(x)} + \frac{\rho^{i}_{aA}(x)}{\rho^{i-1}_{aA}(x)} + \frac{\rho^{i}_{aB}(x)}{\rho^{i+1}_{aB}(x)} - 4 \quad (10)$$

The TSG transformation has the same basic properties as the G transformation and it becomes zero for a homogeneous or 1-D subsurface. In the next paragraphs, we compare the results of G and TSG transformations for some synthetic models and for an archaeological field survey.

## TESTS ON SYNTHETIC DATA

Synthetic data were calculated using a custom built 2-D finite element (F.E.M.) modelling program for the two-sided three-electrode configuration. This program was constructed on the basis of the algorithm published by Uchida and Murakami (1990), Uchida (1991).

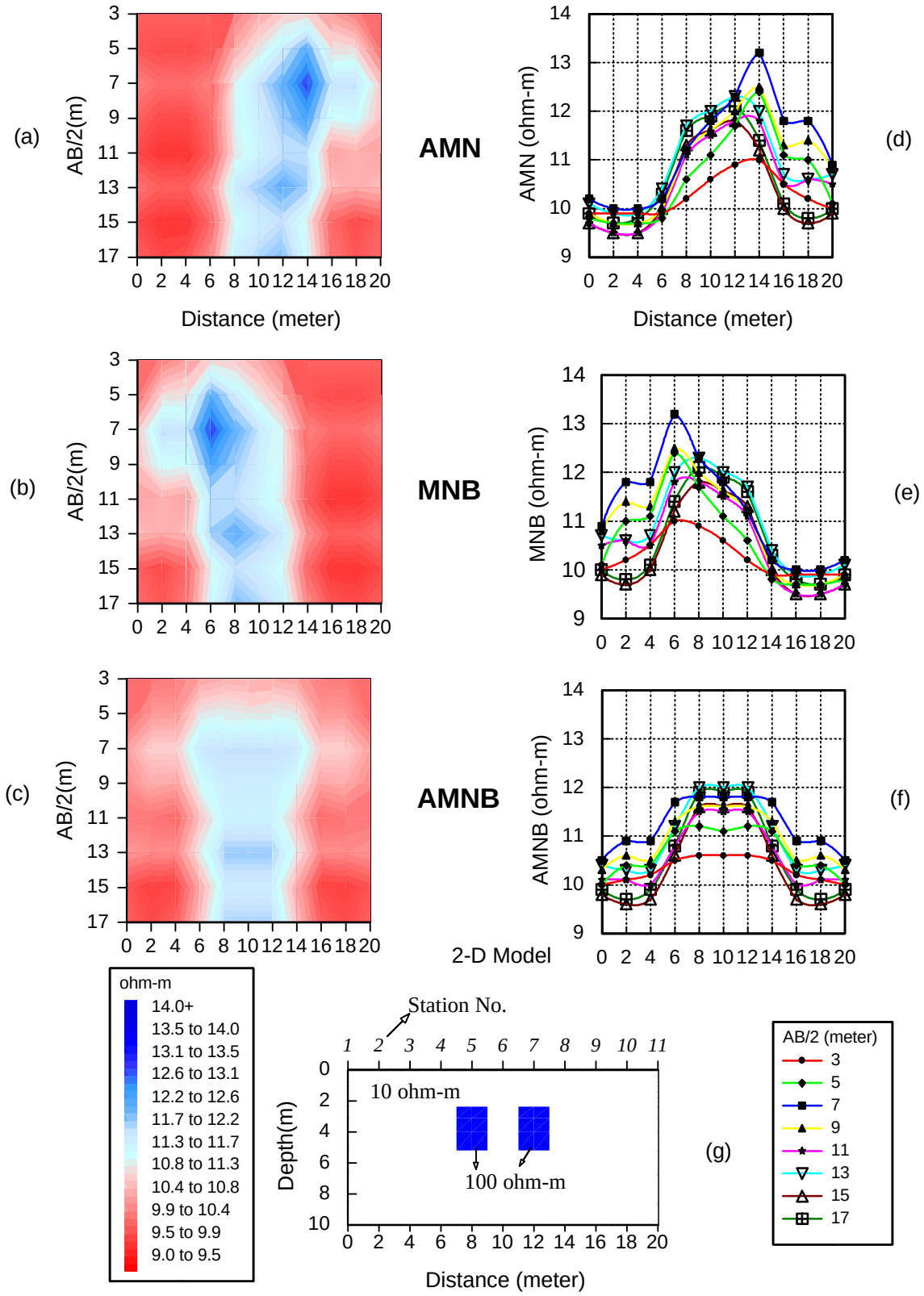


**FIG. 3.** Apparent resistivity pseudosections (left-hand side) and the variation of the apparent resistivity data versus distance (right-hand side). Computations have been performed for AMN (a and d), BMN (b and e) and AMNB (c and f) configurations, respectively. The model consists of two buried resistive targets in a homogenous medium.

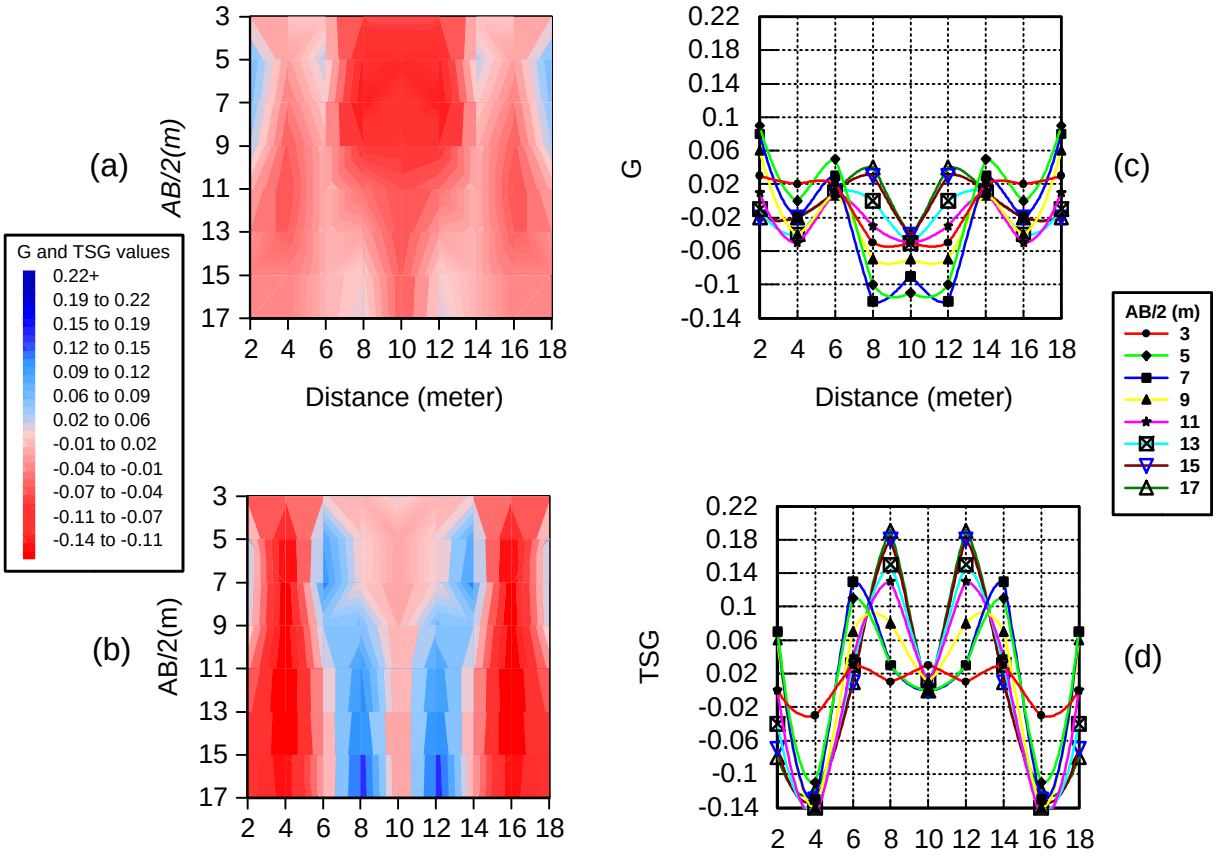


**FIG. 4.** Pseudosection and profiling curves for the G transformation (a) and (c), and for the TSG transformation (b) and (d), respectively, for the model shown in Figure 3g.

A 2-D model of square cross-section is shown in Figure 2c. The model has resistivity of 100 ohm-m and it is hosted in a homogenous half-space of resistivity of 10 ohm-m. The apparent resistivity values calculated for $\overline{AO} = \overline{BO}$ =13 m and MN=2 m are shown in Figure 2a. A comparison of G and TSG transformations is given in Figure 2b. Both transformations show three maxima. However, the numerical value of the central maximum of the G transformation is less than the magnitude of the other two maxima. Consequently, the location of the target body can not be determined correctly using the G transformation. On the contrary, the TSG transformation is more successful in pointing out the location, for this particular model.

The second model consists of two closely located 2-D prisms buried at 2 m depth in a homogenous medium (Fig. 3g). The resistivity value of the prisms is 100 ohm-m. The width and the depth extent of the buried targets are 2 m and 2.7 m, respectively. The resistivity of the surrounding medium is 10 ohm-m. This model could simulate the foundation walls of an ancient construction. The apparent resistivity values have been computed for $\overline{AO} = \overline{BO}$ = 3, 5, 7, 9, 11, 13, 15 and 17 m (n = 1 to n = 8) while the distance between potential electrodes was 2 m (a=2 m). The station spacing was also equal to 2 m.

The apparent resistivity pseudosections, as well as the graphs of the apparent resistivity values calculated for a variety of electrode spacings versus distance, are illustrated in the left- and right-hand side panels of Figure 3, respectively. The top, central and bottom panels show apparent resistivity values corresponding to the AMN, BMN and AMNB configurations. The effect of the targets can not be resolved only by the qualitative interpretation of the apparent resistivity data. Figure 4 shows the results of G and TSG transformations. The existence of the two targets is very clear in the TSG transformation image and its positive numerical values indicate that the resistivity of the targets is higher than that of the surrounding medium.

## ACTUAL FIELD APPLICATION

The real data were collected from the archaeological site known as Alacahoyuk, in the northeastern part of central Turkey. The archaeological site consists of four cultural periods, Calcolitithic

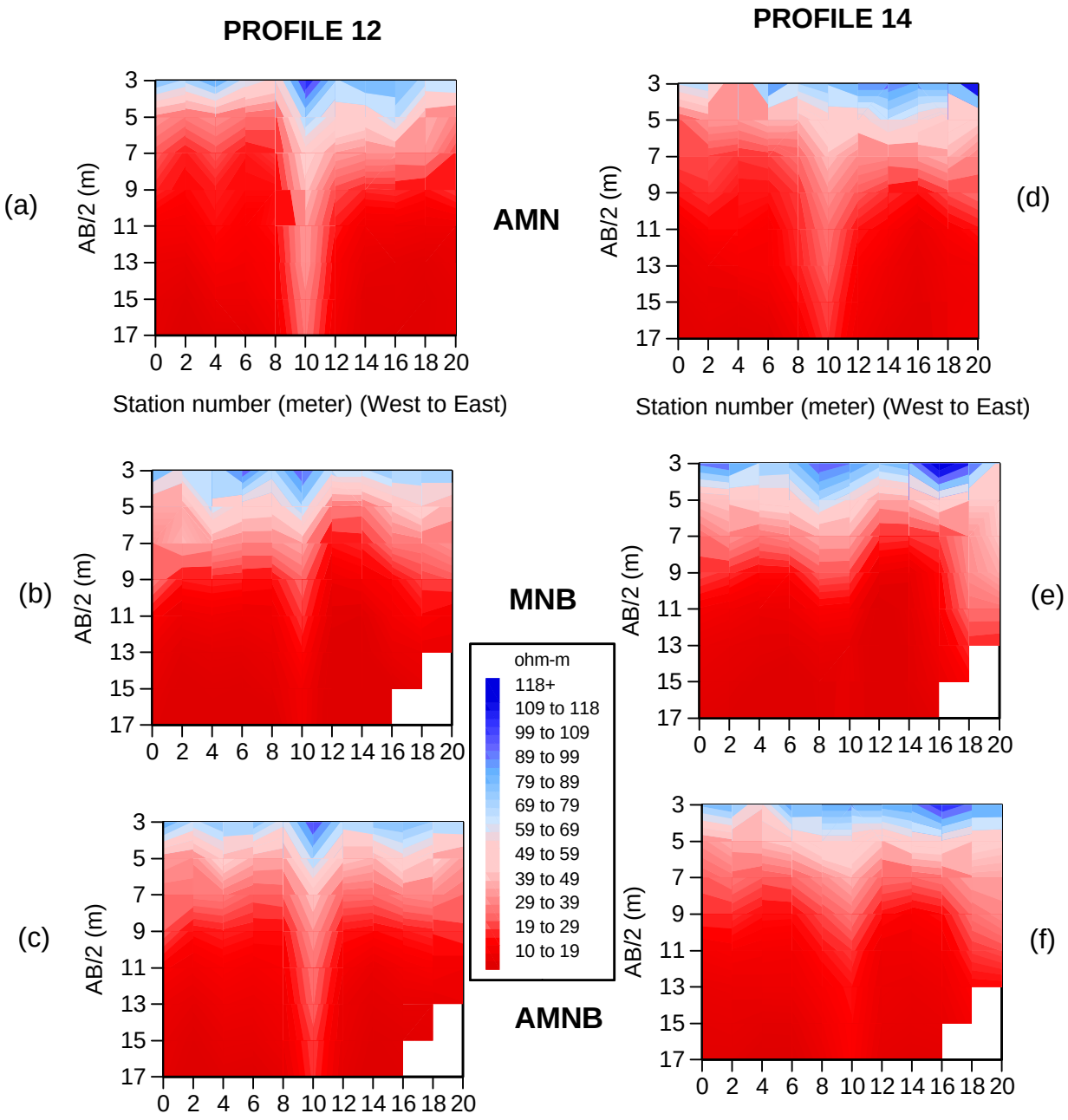


**FIG. 5.** Pseudosection presentations of the apparent resistivity data measured at the Alacahoyuk archaeological site. The left- and right-hand side panels show the data measured on the profiles 12 and 14, respectively. The type of electrode configuration is shown between the columns.

(3500-3000 BC), early Bronze Age (3000-2000 BC), Hittite (2000-1200 BC) and Phrygian. In the Hittite period, the site was an important religious centre surrounded by a city-wall. The location of this wall was not known and the geophysical survey aimed exactly to locate it.

Based on archaeological information, an area having dimensions of 20x28 m was selected for detailed investigations. The terrain was occupied by an abandoned village built on the archaeological site. The inhabitants of this village were moved to another place by the state authorities in 1935. Therefore, the resistivity of the cover was expected to have high values. The buried wall was expected to strike along the north – south direction and to be buried at a depth of about 2-4 m.

The measurements were performed over 15 parallel lines, 20 m long each, and spaced 2 m apart each from the other. The distance between stations was also set to 2 m, thus there were 11 measuring stations along each survey line. The measurement direction was selected to be from west to east and the

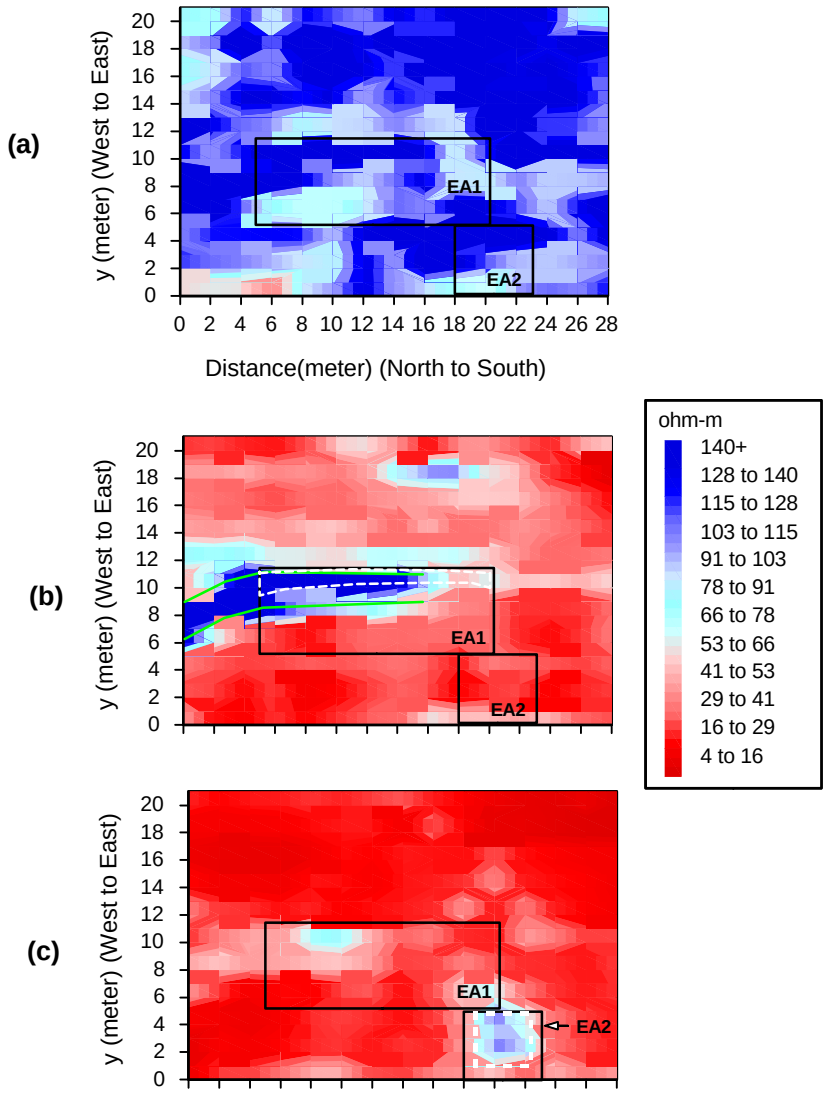


**FIG. 6.** The plan views of the final model inverted from the two-sided three-electrode apparent resistivity data measured at the Alacahoyuk archaeological site. Figure shows the variation of the intrinsic resistivity values inside the blocks that occupy the same depth range. The resistivity maps correspond to the depth ranges 0.41-1.83 (a), 1.83-3.11 (b), 3.11-5.20 (c), respectively. The excavation areas are enclosed by rectangles (EA1 and EA2). White dashed lines indicate the exposed wall and room (after Candansayar and Basokur, 2000).

current electrodes A and B were located on the western and eastern side of the array centre, respectively.

Figure 5 shows representative apparent resistivity pseudosections for profiles 12 and 14. The qualitative interpretation is difficult and it gives impression that an undulating resistive top layer overlies a conductive basement.

Candansayar and Basokur (2000) applied 2-D inversion to the apparent resistivity data for all profiles. The results of the 2-D inversion were presented as resistivity maps by contouring the resistivity values of blocks, which correspond to the same depth range. The purpose of this type of presentation is to examine the lateral resistivity variations in a specified depth. Figure 6a shows the resistivity distribution for the blocks that lie in the depth range between 0.41 m and 1.83 m. This depth range is represented by high resistivity values and thus, it is interpreted as the effect of the covering soil. Figure 6b illustrates the block depths ranging from 1.83 m to 3.11 m. The existence of the wall is clearly indicated in this depth range. This image allows also depth estimates to be done. The estimated depths of the top and bottom of the target are 1.83 m and 3.11 m, respectively. The examination of the highly resistive zone suggests that the wall exist from the first profile till the profile 16. The expected width of the target is 2 m as inferred from the Figure 6b. The area enclosed by a rectangular (EA1) in Figure 6 ser-

**FIG. 7.** A view of the exposed city-wall from the southern side (EA1).

ves as a check of the validity of the interpretation.

The resistivity distribution in the next block range (3.11-5.2) is shown in the Figure 6c. The resistivity values vary monotonously except in a high resistivity zone at southwest of the survey area. The monotonous resistivity variation indicates that the bottom of the wall is limited inside the block of the depth range 1.83-3.11 m. However, the high resistivity zone between profiles 18 and 22 may indicate the existence of a new building having dimensions of 5x5 meters (marked as EA2). The depth of the top and bottom of the building may be estimated from the resistivity image as being 3.11 and 5.2 meters, respectively. Note that all these estimations are limited by the block sizes, which are prescribed by the available computing facilities.

The area EA1 was excavated one year after the geophysical survey. A sketch of the excavated wall is plotted in Figure 6b by white dashed lines. The Archaeologists dated this wall as belonging to Stratum II that corresponds to 2000-1200 BC, the period of the Hitite Empire. The width of the wall varies between 2.5 and 0.5 meters from north to south (Fig. 7). The direction change in the left-hand side of the excavated area is also well estimated from the 2D inversion of the two-sided three-electrode data. But, the exposed wall is continuous throughout the excavation area although the termination of the wall at 16 meters is expected from the 2D inversion of three-electrode array. This could be explained by the dimensional change in the size of the wall. It becomes thinner towards its southern side and both width and depth extent of the wall decrease to 0.5 m (see Fig. 7).

The area EA2 was excavated two years later than the geophysical survey. The exposed building is a room having a big kiln (Fig. 8). The 2-D inversion was very successful in determining the location, depth and size of the room.

Figure 9a and 9b show the G and TSG transformations, respectively, for profiles 12 and 14. The transformation methods eliminate the effect of the 1-D earth and the targets below the high resistive cover layer become visible. Both transformation methods locate successfully the wall in Profile 12. However, the G transformation is not successful in

**FIG. 8.** A view of the exposed room and kiln (EA2).

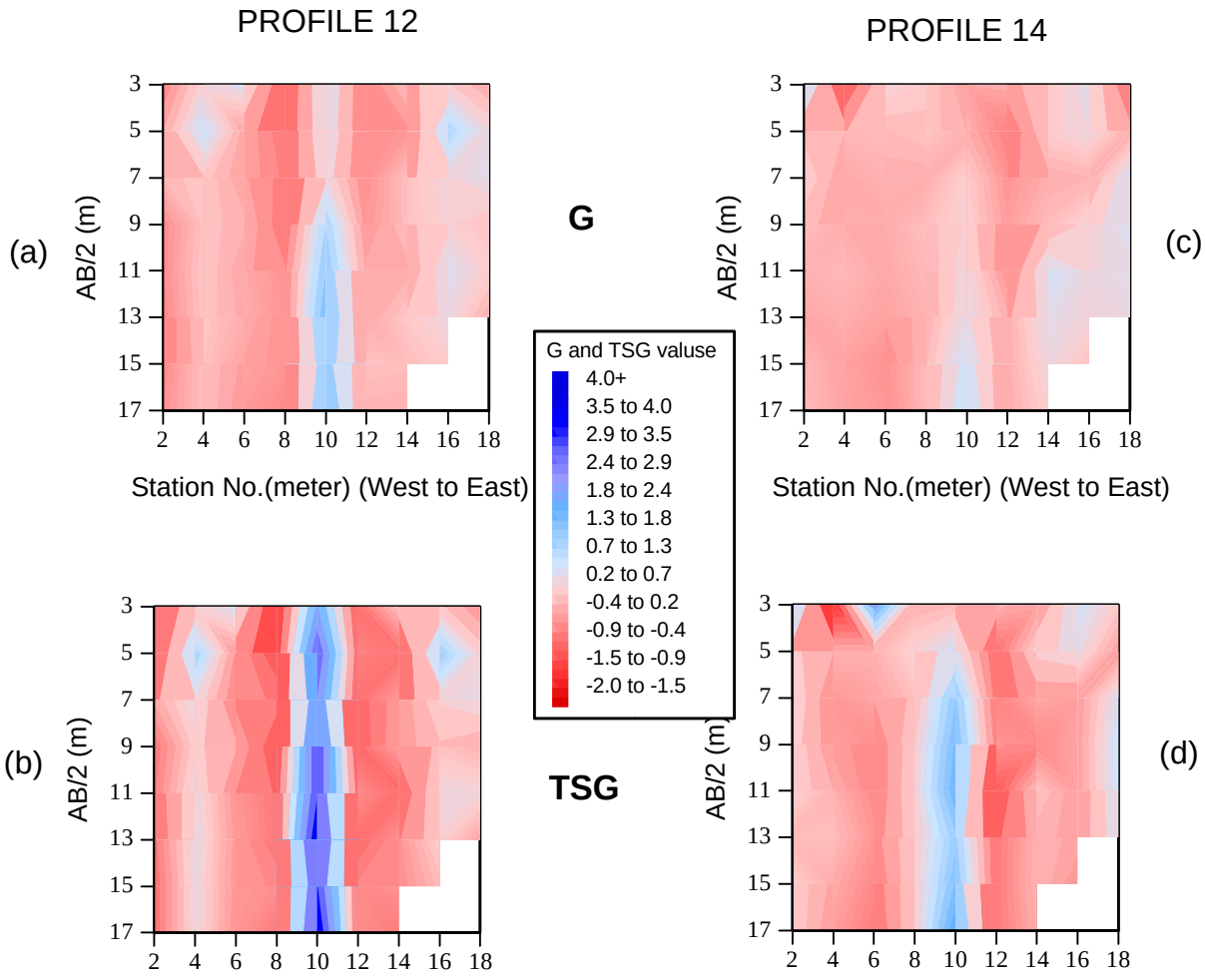


**FIG. 9.** Pseudosection presentations of the G and TSG transformations for profiles 12 (a and b) and 14 (c and d).

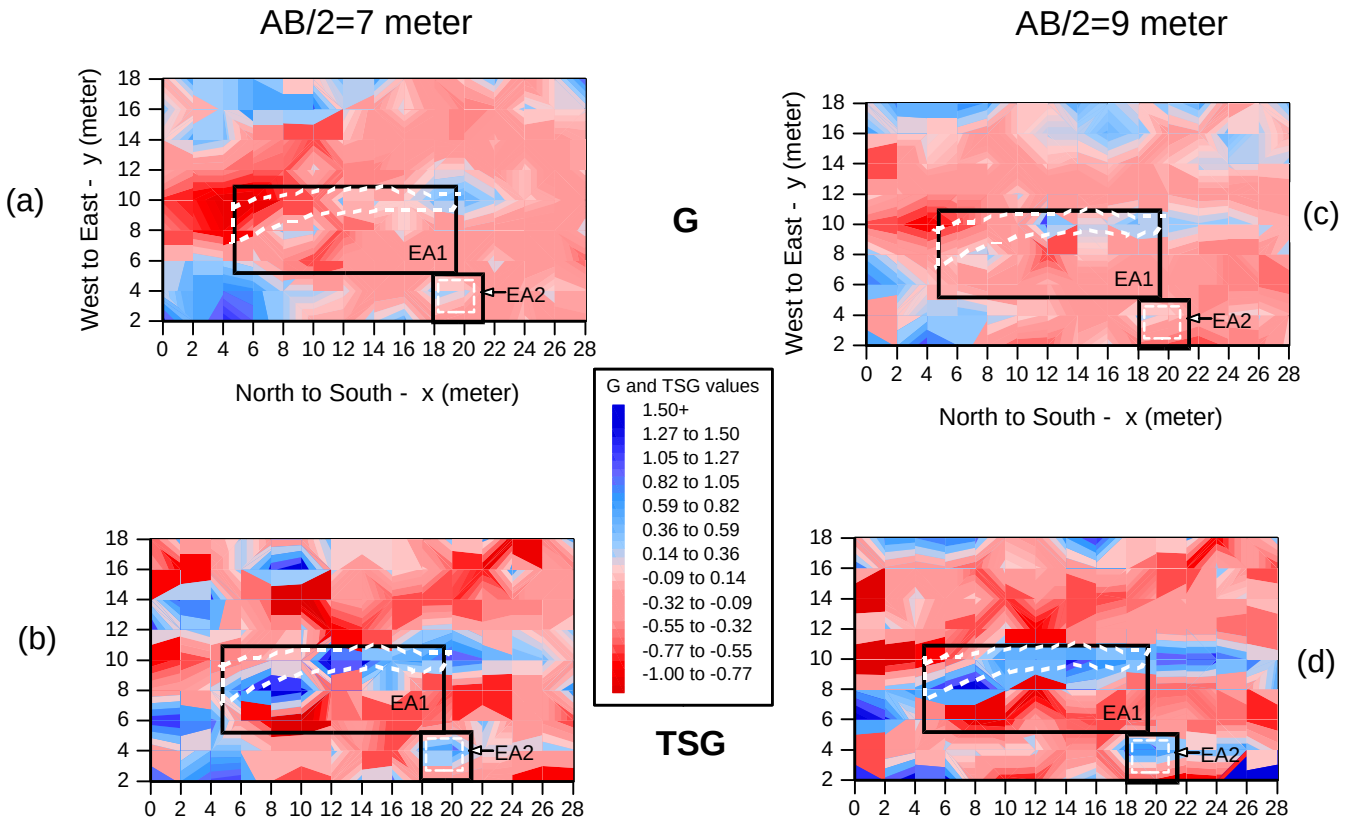


**FIG. 10.** The G (a and c) and TSG (b and d) transformation maps of the survey area. White dashed lines indicate the exposed wall and room.

Profile 14 and in some other profiles. Figure 10 illustrates the G and TSG transformations maps for AB/2=7 and 9 meters. Figures 10c and 10d show that the TSG transformation maps clearly indicate the location and the extension of the exposed wall throughout the excavation area. Moreover, the G transformation failed to give indications for the buried room and the kiln in the excavated area EA2. The TSG transformation provides some information about the existence of the exposed room.

## CONCLUSIONS

The TSG transformation is an efficient tool in delineating shallow lateral discontinuities and it is superior to the G transformation. The extra terms of the TSG transformation improve the sensitivity of the transformation process. The synthetic tests and the results of an actual field survey which were followed by archaeological excavation show that the location of a buried target can be delineated by the use of TSG transformation. However, the TSG transformation could not yield a clear picture of the limit the bottom of the target. Also, the dimensions of a target could not be estimated by the TSG transformation. The 2-D (or 3-D) inversion of the apparent resistivity becomes necessary if one wants to make a quantitative interpretation. However, the TSG transformation derived for two-sided three-electrode configuration is a very fast method and it gives valuable information for the preliminary interpretation the apparent resistivity data.

Moreover, the TSG transformation is very helpful in two-dimensional mesh design. Since the TSG transformation indicates approximately the location of target bodies, then the 2-D modelling mesh could be densely subdivided into relatively small blocks in the vicinity of the disturbing targets. This improves the correctness of calculated model responses and consequently the results of the 2-D inversion.

## ACKNOWLEDGMENT

This paper is a part of MSc thesis of M. E. Candansayar and it was supported by the Scientific and Technical Research Council of Turkey (TUBITAK) under grant no. YDABCAG-553. We thank Prof. Dr. Aykut Cinaroglu, the chief archaeologist of the Alacahoyuk excavation, for his continues contributions and interests. We also thank Gregory N. Tsokas, for his valuable comments and suggestions.

## REFERENCES


Bernabini M., Brizzolari E. and Piro S., 1988, Improvement of signal to noise ratio in resistivity profiles: Geophysical Prospecting, **36**, 559-570.

Brizzolari, E., Samir, A., Orlando, L., Piro, S. and Versino, L., 1989, Filtering and crosscorrelating of resistivity profiles: Boll. Teor. Appl., **16**, 245-257.

Brizzolari, E., Ermolli, F., Orlando, L., Piro, S., and Versino, L., 1992, Integrated geophysical methods in archaeological surveys: Journal of Applied Geophysics, **29**, 47-55.

Candansayar, M. E. and Basokur, A. T., 2000, Detecting small-scale targets by the 2D inversion of two-sided three-electrode data: application to an archaeological survey (submitted to Geophysical Prospecting).

Dahlin, T., 1996, 2D resistivity surveying for environmental and engineering applications: First Break, **14**, 275-283.

Griffiths, D. H. and Barker, R. D., 1994, Electrical imaging in archaeology: Journal of Archaeological Science, **21**, 153-158.

Kampke, A. 1999, Focused imaging of electrical resistivity data in archaeological prospecting: Journal of Applied Geophysics, **41**, 215-227.

Karous, M. and Pernu, T. K., 1985, Combined sounding profiling resistivity measurements with the three-electrode arrays: Geophysical Prospecting, **33**, 447-459.

Noel, M. and Walker, R., 1990, Development of an electrical resistivity tomography system for imaging archaeological structures: Archaeometry '90, Pernicka E. and Wagner G.A. (eds.), Birkhauser, Basel, 767-776.

Noel, M. and Xu, B., 1991, Archaeological investigation by electrical resistivity tomography: Geophysical Journal International, 107, 95-102.

Orlando, L., Piro, S. and Versino, V., 1987, Location of sub-surface geoelectric anomalies for archaeological work: a comparison between experimental arrays and interpretation using numerical methods: Geoexploration, **24,** 227-237.

Schulz, R. and Tezkan, B., 1988, Interpretation of Resistivity measurements over 2D structures: Geophysical Prospecting, **36**, 962-975.

Tsokas, N. G. and Tsourlos, P. I., 1997, Transformation of the resistivity anomalies from archaeological sites by inversion filtering: Geophysics, **62,** 36-43.

Uchida, T. and Murakami, Y., 1990, Development of Fortran Code for the Two-Dimensional Schlumberger Inversion: Geological Survey of Japan (Report).

Uchida, T., 1991, Two-dimensional resistivity inversion for Schlumberger sounding, Geophys. Explor. (Butsuri-Tansa), **44**, 1-17.

van Overmeeren, R. A. and Ritsema, I. L., 1988, Continuous vertical electrical sounding: First Break, **6,** 313-324.